1-1-2005

Search for Lambda$_b^0$-->ppi and Lambda$_b^0$-->pK decays in p [overline p] collisions at sqrt(s)=1.96 TeV

Darin Acosta
University of Florida, acosta@phys.ufl.edu

Kenneth A. Bloom
University of Nebraska-Lincoln, kbloom2@unl.edu

Collider Detector at Fermilab Collaboration

PHYSICAL REVIEW D **72,** 051104(R) (2005)

Search for $\Lambda_b^0 \to p\pi$ and $\Lambda_b^0 \to pK$ decays in $p\bar{p}$ collisions at $\sqrt{s} = 1.96$ TeV

D. Acosta,[16] J. Adelman,[12] T. Affolder,[9] T. Akimoto,[54] M. G. Albrow,[15] D. Ambrose,[15] S. Amerio,[42] D. Amidei,[33] A. Anastassov,[50] K. Anikeev,[15] A. Annovi,[44] J. Antos,[1] M. Aoki,[54] G. Apollinari,[15] T. Arisawa,[56] J-F. Arguin,[32] A. Artikov,[13] W. Ashmanskas,[15] A. Attal,[7] F. Azfar,[41] P. Azzi-Bacchetta,[42] N. Bacchetta,[42] H. Bachacou,[28] W. Badgett,[15] A. Barbaro-Galtieri,[28] G. J. Barker,[25] V. E. Barnes,[46] B. A. Barnett,[24] S. Baroiant,[6] G. Bauer,[31] F. Bedeschi,[44] S. Behari,[24] S. Belforte,[53] G. Bellettini,[44] J. Bellinger,[58] A. Belloni,[31] E. Ben-Haim,[15] D. Benjamin,[14] A. Beretvas,[15] T. Berry,[29] A. Bhatti,[48] M. Binkley,[15] D. Bisello,[42] M. Bishai,[15] R. E. Blair,[2] C. Blocker,[5] K. Bloom,[33] B. Blumenfeld,[24] A. Bocci,[48] A. Bodek,[47] G. Bolla,[46] A. Bolshov,[31] D. Bortoletto,[46] J. Boudreau,[45] S. Bourov,[15] B. Brau,[9] C. Bromberg,[34] E. Brubaker,[12] J. Budagov,[13] H. S. Budd,[47] K. Burkett,[15] G. Busetto,[42] P. Bussey,[19] K. L. Byrum,[2] S. Cabrera,[14] M. Campanelli,[18] M. Campbell,[33] F. Canelli,[7] A. Canepa,[46] M. Casarsa,[53] D. Carlsmith,[58] R. Carosi,[44] S. Carron,[14] M. Cavalli-Sforza,[3] A. Castro,[4] P. Catastini,[44] D. Cauz,[53] A. Cerri,[28] L. Cerrito,[41] J. Chapman,[33] Y. C. Chen,[1] M. Chertok,[6] G. Chiarelli,[44] G. Chlachidze,[13] F. Chlebana,[15] I. Cho,[27] K. Cho,[27] D. Chokheli,[13] J. P. Chou,[20] S. Chuang,[58] K. Chung,[11] W-H. Chung,[58] Y. S. Chung,[47] M. Ciljak,[44] C. I. Ciobanu,[23] M. A. Ciocci,[44] A. G. Clark,[18] D. Clark,[5] M. Coca,[14] A. Connolly,[28] M. Convery,[48] J. Conway,[6] B. Cooper,[30] K. Copic,[33] M. Cordelli,[17] G. Cortiana,[42] J. Cranshaw,[52] J. Cuevas,[10] A. Cruz,[16] R. Culbertson,[15] C. Currat,[28] D. Cyr,[58] D. Dagenhart,[5] S. Da Ronco,[42] S. D'Auria,[19] P. de Barbaro,[47] S. De Cecco,[49] A. Deisher,[28] G. De Lentdecker,[47] M. Dell'Orso,[44] S. Demers,[47] L. Demortier,[48] M. Deninno,[4] D. De Pedis,[49] P. F. Derwent,[15] C. Dionisi,[49] J. R. Dittmann,[15] P. DiTuro,[50] C. Dörr,[25] A. Dominguez,[28] S. Donati,[44] M. Donega,[18] J. Donini,[42] M. D'Onofrio,[18] T. Dorigo,[42] K. Ebina,[56] J. Efron,[38] J. Ehlers,[18] R. Erbacher,[6] M. Erdmann,[25] D. Errede,[23] S. Errede,[23] R. Eusebi,[47] H-C. Fang,[28] S. Farrington,[29] I. Fedorko,[44] W. T. Fedorko,[12] R. G. Feild,[59] M. Feindt,[25] J. P. Fernandez,[46] R. D. Field,[16] G. Flanagan,[34] L. R. Flores-Castillo,[45] A. Foland,[20] S. Forrester,[6] G. W. Foster,[15] M. Franklin,[20] J. C. Freeman,[28] Y. Fujii,[26] I. Furic,[12] A. Gajjar,[29] M. Gallinaro,[48] J. Galyardt,[11] M. Garcia-Sciveres,[28] A. F. Garfinkel,[46] C. Gay,[59] H. Gerberich,[14] D. W. Gerdes,[33] E. Gerchtein,[11] S. Giagu,[49] P. Giannetti,[44] A. Gibson,[28] K. Gibson,[11] C. Ginsburg,[15] K. Giolo,[46] M. Giordani,[53] M. Giunta,[44] G. Giurgiu,[11] V. Glagolev,[13] D. Glenzinski,[15] M. Gold,[36] N. Goldschmidt,[33] D. Goldstein,[7] J. Goldstein,[41] G. Gomez,[10] G. Gomez-Ceballos,[10] M. Goncharov,[51] O. González,[46] I. Gorelov,[36] A. T. Goshaw,[14] Y. Gotra,[45] K. Goulianos,[48] A. Gresele,[42] M. Griffiths,[29] C. Grosso-Pilcher,[12] U. Grundler,[23] J. Guimaraes da Costa,[20] C. Haber,[28] K. Hahn,[43] S. R. Hahn,[15] E. Halkiadakis,[47] A. Hamilton,[32] B-Y. Han,[47] R. Handler,[58] F. Happacher,[17] K. Hara,[54] M. Hare,[55] R. F. Harr,[57] R. M. Harris,[15] F. Hartmann,[25] K. Hatakeyama,[48] J. Hauser,[7] C. Hays,[14] H. Hayward,[29] B. Heinemann,[29] J. Heinrich,[43] M. Hennecke,[25] M. Herndon,[24] C. Hill,[9] D. Hirschbuehl,[25] A. Hocker,[15] K. D. Hoffman,[12] A. Holloway,[20] S. Hou,[1] M. A. Houlden,[29] B. T. Huffman,[41] Y. Huang,[14] R. E. Hughes,[38] J. Huston,[34] K. Ikado,[56] J. Incandela,[9] G. Introzzi,[44] M. Iori,[49] Y. Ishizawa,[54] C. Issever,[9] A. Ivanov,[6] Y. Iwata,[22] B. Iyutin,[31] E. James,[15] D. Jang,[50] B. Jayatilaka,[33] D. Jeans,[49] H. Jensen,[15] E. J. Jeon,[27] M. Jones,[46] K. K. Joo,[27] S. Y. Jun,[11] T. Junk,[23] T. Kamon,[51] J. Kang,[33] M. Karagoz Unel,[37] P. E. Karchin,[57] Y. Kato,[40] Y. Kemp,[25] R. Kephart,[15] U. Kerzel,[25] V. Khotilovich,[51] B. Kilminster,[38] D. H. Kim,[27] H. S. Kim,[23] J. E. Kim,[27] M. J. Kim,[11] M. S. Kim,[27] S. B. Kim,[27] S. H. Kim,[54] Y. K. Kim,[12] M. Kirby,[14] L. Kirsch,[5] S. Klimenko,[16] M. Klute,[31] B. Knuteson,[31] B. R. Ko,[14] H. Kobayashi,[54] D. J. Kong,[27] K. Kondo,[56] J. Konigsberg,[16] K. Kordas,[32] A. Korn,[31] A. Korytov,[16] A. V. Kotwal,[14] A. Kovalev,[43] J. Kraus,[23] I. Kravchenko,[31] A. Kreymer,[15] J. Kroll,[43] M. Kruse,[14] V. Krutelyov,[51] S. E. Kuhlmann,[2] S. Kwang,[12] A. T. Laasanen,[46] S. Lai,[32] S. Lami,[44] S. Lammel,[15] M. Lancaster,[30] R. Lander,[6] K. Lannon,[38] A. Lath,[50] G. Latino,[44] I. Lazzizzera,[42] C. Lecci,[25] T. LeCompte,[2] J. Lee,[27] J. Lee,[47] S. W. Lee,[51] R. Lefèvre,[3] N. Leonardo,[31] S. Leone,[44] S. Levy,[12] J. D. Lewis,[15] K. Li,[59] C. Lin,[59] C. S. Lin,[15] M. Lindgren,[15] E. Lipeles,[8] T. M. Liss,[23] A. Lister,[18] D. O. Litvintsev,[15] T. Liu,[15] Y. Liu,[18] N. S. Lockyer,[43] A. Loginov,[35] M. Loreti,[42] P. Loverre,[49] R-S. Lu,[1] D. Lucchesi,[42] P. Lujan,[28] P. Lukens,[15] G. Lungu,[16] L. Lyons,[41] J. Lys,[28] R. Lysak,[1] E. Lytken,[46] D. MacQueen,[32] R. Madrak,[15] K. Maeshima,[15] P. Maksimovic,[24] G. Manca,[29] F. Margaroli,[4] R. Marginean,[15] C. Marino,[23] A. Martin,[59] M. Martin,[24] V. Martin,[37] M. Martínez,[3] T. Maruyama,[54] H. Matsunaga,[54] M. Mattson,[57] P. Mazzanti,[4] K. S. McFarland,[47] D. McGivern,[30] P. M. McIntyre,[51] P. McNamara,[50] R. McNulty,[29] A. Mehta,[29] S. Menzemer,[31] A. Menzione,[44] P. Merkel,[46] C. Mesropian,[48] A. Messina,[49] T. Miao,[15] N. Miladinovic,[5] J. Miles,[31] L. Miller,[20] R. Miller,[34] J. S. Miller,[33] C. Mills,[9] R. Miquel,[28] S. Miscetti,[17] G. Mitselmakher,[16] A. Miyamoto,[26] N. Moggi,[4] B. Mohr,[7] R. Moore,[15] M. Morello,[44] P. A. Movilla Fernandez,[28] J. Muelmenstaedt,[28] A. Mukherjee,[15] M. Mulhearn,[31] T. Muller,[25] R. Mumford,[24] A. Munar,[43] P. Murat,[15] J. Nachtman,[15] S. Nahn,[59] I. Nakano,[39] A. Napier,[55] R. Napora,[24] D. Naumov,[36] V. Necula,[16] T. Nelson,[15] C. Neu,[43] M. S. Neubauer,[8] J. Nielsen,[28] T. Nigmanov,[45] L. Nodulman,[2] O. Norniella,[3] T. Ogawa,[56] S. H. Oh,[14] Y. D. Oh,[27] T. Ohsugi,[22] T. Okusawa,[40] R. Oldeman,[29] R. Orava,[21] W. Orejudos,[28] K. Osterberg,[21] C. Pagliarone,[44] E. Palencia,[10]

R. Paoletti,[44] V. Papadimitriou,[15] A. A. Paramonov,[12] S. Pashapour,[32] J. Patrick,[15] G. Pauletta,[53] M. Paulini,[11] C. Paus,[31] D. Pellett,[6] A. Penzo,[53] T. J. Phillips,[14] G. Piacentino,[44] J. Piedra,[10] K. T. Pitts,[23] C. Plager,[7] L. Pondrom,[58] G. Pope,[45] X. Portell,[3] O. Poukhov,[13] N. Pounder,[41] F. Prakoshyn,[13] A. Pronko,[16] J. Proudfoot,[2] F. Ptohos,[17] G. Punzi,[44] J. Rademacker,[41] M. A. Rahaman,[45] A. Rakitine,[31] S. Rappoccio,[20] F. Ratnikov,[50] H. Ray,[33] B. Reisert,[15] V. Rekovic,[36] P. Renton,[41] M. Rescigno,[49] F. Rimondi,[4] K. Rinnert,[25] L. Ristori,[44] W. J. Robertson,[14] A. Robson,[19] T. Rodrigo,[10] S. Rolli,[55] R. Roser,[15] R. Rossin,[16] C. Rott,[46] J. Russ,[11] V. Rusu,[12] A. Ruiz,[10] D. Ryan,[55] H. Saarikko,[21] S. Sabik,[32] A. Safonov,[6] R. St. Denis,[19] W. K. Sakumoto,[47] G. Salamanna,[49] D. Saltzberg,[7] C. Sanchez,[3] L. Santi,[53] S. Sarkar,[49] K. Sato,[54] P. Savard,[32] A. Savoy-Navarro,[15] P. Schlabach,[15] E. E. Schmidt,[15] M. P. Schmidt,[59] M. Schmitt,[37] T. Schwarz,[33] L. Scodellaro,[10] A. L. Scott,[9] A. Scribano,[44] F. Scuri,[44] A. Sedov,[46] S. Seidel,[36] Y. Seiya,[40] A. Semenov,[13] F. Semeria,[4] L. Sexton-Kennedy,[15] I. Sfiligoi,[17] M. D. Shapiro,[28] T. Shears,[29] P. F. Shepard,[45] D. Sherman,[20] M. Shimojima,[54] M. Shochet,[12] Y. Shon,[58] I. Shreyber,[35] A. Sidoti,[44] A. Sill,[52] P. Sinervo,[32] A. Sisakyan,[13] J. Sjolin,[41] A. Skiba,[25] A. J. Slaughter,[15] K. Sliwa,[55] D. Smirnov,[36] J. R. Smith,[6] F. D. Snider,[15] R. Snihur,[32] M. Soderberg,[33] A. Soha,[6] S. V. Somalwar,[50] J. Spalding,[15] M. Spezziga,[52] F. Spinella,[44] P. Squillacioti,[44] H. Stadie,[25] M. Stanitzki,[59] B. Stelzer,[32] O. Stelzer-Chilton,[32] D. Stentz,[37] J. Strologas,[36] D. Stuart,[9] J. S. Suh,[27] A. Sukhanov,[16] K. Sumorok,[31] H. Sun,[55] T. Suzuki,[54] A. Taffard,[23] R. Tafirout,[32] H. Takano,[54] R. Takashima,[39] Y. Takeuchi,[54] K. Takikawa,[54] M. Tanaka,[2] R. Tanaka,[39] N. Tanimoto,[39] M. Tecchio,[33] P. K. Teng,[1] K. Terashi,[48] R. J. Tesarek,[15] S. Tether,[31] J. Thom,[15] A. S. Thompson,[19] E. Thomson,[43] P. Tipton,[47] V. Tiwari,[11] S. Tkaczyk,[15] D. Toback,[51] K. Tollefson,[34] T. Tomura,[54] D. Tonelli,[44] M. Tönnesmann,[34] S. Torre,[44] D. Torretta,[15] S. Tourneur,[15] W. Trischuk,[32] R. Tsuchiya,[56] S. Tsuno,[39] D. Tsybychev,[16] N. Turini,[44] F. Ukegawa,[54] T. Unverhau,[19] S. Uozumi,[54] D. Usynin,[43] L. Vacavant,[28] A. Vaiciulis,[47] A. Varganov,[33] S. Vejcik III,[15] G. Velev,[15] V. Veszpremi,[46] G. Veramendi,[23] T. Vickey,[23] R. Vidal,[15] I. Vila,[10] R. Vilar,[10] I. Vollrath,[32] I. Volobouev,[28] M. von der Mey,[7] P. Wagner,[51] R. G. Wagner,[2] R. L. Wagner,[15] W. Wagner,[25] R. Wallny,[7] T. Walter,[25] Z. Wan,[50] M. J. Wang,[1] S. M. Wang,[16] A. Warburton,[32] B. Ward,[19] S. Waschke,[19] D. Waters,[30] T. Watts,[50] M. Weber,[28] W. C. Wester III,[15] B. Whitehouse,[55] D. Whiteson,[43] A. B. Wicklund,[2] E. Wicklund,[15] H. H. Williams,[43] P. Wilson,[15] B. L. Winer,[38] P. Wittich,[43] S. Wolbers,[15] C. Wolfe,[12] M. Wolter,[55] M. Worcester,[7] S. Worm,[50] T. Wright,[33] X. Wu,[18] F. Würthwein,[8] A. Wyatt,[30] A. Yagil,[15] T. Yamashita,[39] K. Yamamoto,[40] J. Yamaoka,[50] C. Yang,[59] U. K. Yang,[12] W. Yao,[28] G. P. Yeh,[15] J. Yoh,[15] K. Yorita,[56] T. Yoshida,[40] I. Yu,[27] S. Yu,[43] J. C. Yun,[15] L. Zanello,[49] A. Zanetti,[53] I. Zaw,[20] F. Zetti,[44] J. Zhou,[50] and S. Zucchelli[4]

(CDF Collaboration)

[1]*Institute of Physics, Academia Sinica, Taipei, Taiwan 11529, Republic of China*
[2]*Argonne National Laboratory, Argonne, Illinois 60439, USA*
[3]*Institut de Fisica d'Altes Energies, Universitat Autonoma de Barcelona, E-08193, Bellaterra (Barcelona), Spain*
[4]*Istituto Nazionale di Fisica Nucleare, University of Bologna, I-40127 Bologna, Italy*
[5]*Brandeis University, Waltham, Massachusetts 02254, USA*
[6]*University of California, Davis, Davis, California 95616, USA*
[7]*University of California, Los Angeles, Los Angeles, California 90024, USA*
[8]*University of California, San Diego, La Jolla, California 92093, USA*
[9]*University of California, Santa Barbara, Santa Barbara, California 93106, USA*
[10]*Instituto de Fisica de Cantabria, CSIC-University of Cantabria, 39005 Santander, Spain*
[11]*Carnegie Mellon University, Pittsburgh, Pennsylvania 15213, USA*
[12]*Enrico Fermi Institute, University of Chicago, Chicago, Illinois 60637, USA*
[13]*Joint Institute for Nuclear Research, RU-141980 Dubna, Russia*
[14]*Duke University, Durham, North Carolina 27708, USA*
[15]*Fermi National Accelerator Laboratory, Batavia, Illinois 60510, USA*
[16]*University of Florida, Gainesville, Florida 32611, USA*
[17]*Laboratori Nazionali di Frascati, Istituto Nazionale di Fisica Nucleare, I-00044 Frascati, Italy*
[18]*University of Geneva, CH-1211 Geneva 4, Switzerland*
[19]*Glasgow University, Glasgow G12 8QQ, United Kingdom*
[20]*Harvard University, Cambridge, Massachusetts 02138, USA*
[21]*Division of High Energy Physics, Department of Physics, University of Helsinki and Helsinki Institute of Physics, FIN-00014, Helsinki, Finland*
[22]*Hiroshima University, Higashi-Hiroshima 724, Japan*

[23]*University of Illinois, Urbana, Illinois 61801, USA*
[24]*The Johns Hopkins University, Baltimore, Maryland 21218, USA*
[25]*Institut für Experimentelle Kernphysik, Universität Karlsruhe, 76128 Karlsruhe, Germany*
[26]*High Energy Accelerator Research Organization (KEK), Tsukuba, Ibaraki 305, Japan*
[27]*Center for High Energy Physics: Kyungpook National University, Taegu 702-701;*
Seoul National University, Seoul 151-742;
and SungKyunKwan University, Suwon 440-746; Korea
[28]*Ernest Orlando Lawrence Berkeley National Laboratory, Berkeley, California 94720, USA*
[29]*University of Liverpool, Liverpool L69 7ZE, United Kingdom*
[30]*University College London, London WC1E 6BT, United Kingdom*
[31]*Massachusetts Institute of Technology, Cambridge, Massachusetts 02139, USA*
[32]*Institute of Particle Physics: McGill University, Montréal, Canada H3A 2T8;*
and University of Toronto, Toronto, Canada M5S 1A7
[33]*University of Michigan, Ann Arbor, Michigan 48109, USA*
[34]*Michigan State University, East Lansing, Michigan 48824, USA*
[35]*Institution for Theoretical and Experimental Physics, ITEP, Moscow 117259, Russia*
[36]*University of New Mexico, Albuquerque, New Mexico 87131, USA*
[37]*Northwestern University, Evanston, Illinois 60208, USA*
[38]*The Ohio State University, Columbus, Ohio 43210, USA*
[39]*Okayama University, Okayama 700-8530, Japan*
[40]*Osaka City University, Osaka 588, Japan*
[41]*University of Oxford, Oxford OX1 3RH, United Kingdom*
[42]*University of Padova, Istituto Nazionale di Fisica Nucleare, Sezione di Padova-Trento, I-35131 Padova, Italy*
[43]*University of Pennsylvania, Philadelphia, Pennsylvania 19104, USA*
[44]*Istituto Nazionale di Fisica Nucleare Pisa, Universities of Pisa, Siena and Scuola Normale Superiore, I-56127 Pisa, Italy*
[45]*University of Pittsburgh, Pittsburgh, Pennsylvania 15260, USA*
[46]*Purdue University, West Lafayette, Indiana 47907, USA*
[47]*University of Rochester, Rochester, New York 14627, USA*
[48]*The Rockefeller University, New York, New York 10021, USA*
[49]*Istituto Nazionale di Fisica Nucleare, Sezione di Roma 1, University di Roma "La Sapienza," I-00185 Roma, Italy*
[50]*Rutgers University, Piscataway, New Jersey 08855, USA*
[51]*Texas A&M University, College Station, Texas 77843, USA*
[52]*Texas Tech University, Lubbock, Texas 79409, USA*
[53]*Istituto Nazionale di Fisica Nucleare, University of Trieste, Udine, Italy*
[54]*University of Tsukuba, Tsukuba, Ibaraki 305, Japan*
[55]*Tufts University, Medford, Massachusetts 02155, USA*
[56]*Waseda University, Tokyo 169, Japan*
[57]*Wayne State University, Detroit, Michigan 48201, USA*
[58]*University of Wisconsin, Madison, Wisconsin 53706, USA*
[59]*Yale University, New Haven, Connecticut 06520, USA*
(Received 13 July 2005; published 19 September 2005)

We report on a search for $\Lambda_b^0 \to p\pi^-$ and $\Lambda_b^0 \to pK^-$ (and charge conjugate) decays in $p\bar{p}$ collisions at $\sqrt{s} = 1.96$ TeV using 193 pb^{-1} of data collected by the CDF II experiment at the Fermilab Tevatron Collider. Data were collected using a track trigger that has been optimized to select tracks belonging to a secondary vertex that is typical of two-body charmless decays of b-flavored hadrons, including Λ_b^0 baryons. As no Λ_b^0 signal was observed, we set the upper limits on the branching fraction $\mathcal{B}(\Lambda_b^0 \to ph^-)$, where h is K or π, of 2.3×10^{-5} at 90% C.L. and 2.9×10^{-5} at 95% C.L.

DOI: 10.1103/PhysRevD.72.051104 PACS numbers: 13.30.Eg, 14.20.Mr

Charmless, hadronic b-meson decays have been of great interest because they provide important information on the violation of the combined symmetry operations of charge conjugation (C) and parity (P) in the standard model of electroweak interactions [1,2]. The first observation of charmless hadronic b-meson decays by the CLEO collaboration in 1993 [3], and the subsequent realization that hadronic penguin diagrams dominate some of these decays [4], has since stimulated a substantial body of theoretical work [5–7]. In contrast, our present theoretical and experimental knowledge of the corresponding b-baryon decays is rather limited. Measurements of branching fractions and CP asymmetries for decays like $\Lambda_b^0 \to pK$ or $p\pi$ could provide valuable new insight into the hadronic dynamics of b-hadron decays into charmless final states. In the standard model, the CP-violating rate asymmetries in these decays are expected to be large compared to the corresponding asymmetries in b-meson decays [8–10].

The existence of the Λ_b^0 is well established [11–15], however, no charmless decays have been observed. We search for Λ_b^0 decaying to pK and $p\pi$. Theoretical predictions for their branching ratios lie in the range $(0.9 - 1.2) \times 10^{-6}$ for $p\pi$ decays and $(1.4 - 1.9) \times 10^{-6}$ for pK decays [16]. The current experimental upper limit on the branching ratios of these decay modes has been measured by the ALEPH experiment and is 5×10^{-5} at 90% C.L. [17]. The hadronic b trigger of the upgraded collider detector at Fermilab (CDF II) selects events with track pairs originating from a common displaced vertex. A clean signal of charmless hadronic B decays has been reconstructed using this trigger [18]. The same sample should contain the two-body charmless Λ_b^0 decays in pK and $p\pi$.

This search uses a $193 \pm 12\text{pb}^{-1}$ [19] data sample recorded by the CDF II experiment at the Tevatron $p\bar{p}$ collider with $\sqrt{s} = 1.96$ TeV between February 2002 and September 2003. The components of the CDF II detector pertinent to this analysis are described briefly below. Detailed descriptions can be found elsewhere [20]. Two silicon microstrip detectors SVX II [21] and ISL [22] and a cylindrical drift chamber COT [23], immersed in a 1.4 T solenoidal magnetic field, track charged particles in the range $|\eta| < 1.0$ [24]. The solenoid covers $r < 150$ cm. The SVX II provides up to five $r - \phi$ position measurements, each of $\sim$15 μm precision, at radii between 2.5 cm and 10.6 cm. The ISL provides one axial and one stereo measurement with $\sim$20 μm precision, at radii between 20 cm and 28 cm, helping to connect the tracks in the COT with those in the SVX, and improving the tracking efficiency. The COT has 96 measurement layers, between 40 cm and 137 cm in radius, organized into eight alternating axial and $\pm 2^\circ$ stereo superlayers. An additional silicon detector, L00 [25], at radius of 1.3 cm is present but is not used in this analysis.

The events used are selected with a three-level trigger system. At level 1, charged tracks in the COT transverse plane are reconstructed by a hardware processor (XFT) [26]. The trigger requires two oppositely charged tracks with reconstructed transverse momenta $p_T \geq 2$ GeV/c and $p_{T1} + p_{T2} \geq 5.5$ GeV/c. At level 2, the silicon vertex tracker (SVT) [27] associates SVX II position measurements with XFT tracks. The impact parameter of the track (d_0) with respect to the beam line is measured with 50 μm resolution, which includes a $\sim$30 μm contribution from transverse beam size as measured in SVT. Requiring two tracks with 100 $\mu\text{m} \leq |d_0| \leq 1.0$ mm selects a sample enriched in heavy flavor. The two trigger tracks must have an opening angle between 20° and 135°. The track pair also is required to be consistent with originating from a particle having a transverse decay length larger than 200 μm and an impact parameter less than 140 μm. At level 3, we fully reconstruct the event using the offline software. Candidate trigger tracks are then selected from this improved set of tracks by matching them in curvature and ϕ to tracks reconstructed by the level 2 trigger. To select candidate events, the Level 1 and Level 2 selections are then applied to the set of matched tracks, and the invariant mass, assuming the tracks are pions, is required to be within 4 and 7 GeV/c^2.

We normalize the $\Lambda_b^0 \to ph^-$ branching ratio to the branching ratio $\mathcal{B}(B_d^0 \to K\pi) = (1.85 \pm 0.11) \times 10^{-5}$ [28]. The normalization mode has been chosen because its decay topology is similar to that of the signal. The normalization mode is not well separated from the other $B \to h^+h'^-$ decays at CDF, namely, $B_d^0 \to \pi\pi$, $B_s^0 \to K\pi$, and $B_s^0 \to KK$. To obtain the yield of $B_d^0 \to K\pi$ we measure the overall $B \to h^+h'^-$ yield and then fit the relative fraction $R = N(B_d^0 \to K\pi)/N(B \to h^+h'^-)$ using an unbinned maximum likelihood fit [18]. The likelihood function has contributions from the signal ($B \to h^+h'^-$) and the background. The signal likelihood is given by the six distinct $B_{s,d}^0$ decays modes into KK, $\pi\pi$, and $K^\pm\pi^\mp$. In addition to $M_{\pi\pi}$, the kinematic variable used is the charged-signed momentum imbalance, defined as $\alpha = (1 - \frac{p_1}{p_2}) \cdot q_1$, where the $p_1(p_2)$ are the modulus of the smaller (larger) momentum of the tracks, and q_1 is the charge sign of the track assigned to p_1.

The relationship between the number of events (N) and branching ratios ($\mathcal{B}$) of the signal and normalizing mode are given by

$$\mathcal{B}(\Lambda_b^0 \to ph^-) = \frac{N(\Lambda_b^0 \to ph^-)}{A}, \tag{1}$$

and

$$A = \frac{\epsilon_\Lambda}{\epsilon_B} \cdot \frac{f_\Lambda}{f_d} \cdot \frac{R \cdot N(B \to h^+h'^-)}{\mathcal{B}(B_d^0 \to K\pi)}, \tag{2}$$

where ϵ_Λ (ϵ_B) is the total efficiency for observing a Λ_b^0 (B_d^0) and f_Λ (f_d) is the b-quark hadronization fraction of the Λ_b^0 (B_d^0). We use the following values: $f_\Lambda = 0.099 \pm 0.017$ and $f_d = 0.397 \pm 0.010$ [29]. These mean values are obtained from measurements at both LEP (see [30,31]) and CDF [32], using data samples containing both b baryons and mesons and sensitive to p_T of the Λ_b^0 down to 10 GeV/c. The value of the ratio we use is $f_\Lambda/f_d = 0.25 \pm 0.04$. We estimate the efficiencies using a detailed Monte Carlo simulation of the detector and of the trigger using GEANT [33], to generate samples of Λ_b^0 and B_d^0.

A blind analysis was performed. The data in the signal mass window were hidden and the analysis selections optimized without knowledge of their actual impact on the result. The background was calculated by fitting the invariant mass spectrum and interpolating in the blinded signal region. Only after all selection criteria were fixed and the systematic uncertainties estimated was the signal region unblinded, and the number of events counted and compared with the expected background. Potential biases in the background estimate, introduced by the cut optimi-

zation procedure, were avoided by splitting the full sample into two statistically independent subsamples: one consisting of even event numbers and the other one of odd event numbers. One half of the sample was used for the cut optimization described below; the background level measured on the other half has been multiplied by two to calculate the expected background in the search window.

We select candidate track pairs from the set of offline tracks that match trigger tracks based on invariant mass, impact parameter, and transverse decay length of the track pair, as well as impact parameter of each track. The exact criteria are optimized as discussed below. Figure 1 shows the invariant mass distribution after all selection criteria are applied. The dotted line indicates the region that was blinded during the cut optimization. The solid line indicates the fit region used to determine the expected background level.

We assign the pion mass to all tracks, resulting in slight mass shifts between the various b-hadron decays to two-track final states.

A large Monte Carlo sample including $B \to h^+h'^-$ and $\Lambda_b^0 \to ph^-$ was used to determine the separation of the two mass peaks. For $B \to h^+h'^-$, the mean and rms were 5258 MeV/c^2 and 34 MeV/c^2 . For $\Lambda_b^0 \to ph^-$, the mean and rms were 5454 MeV/c^2 and 60 MeV/c^2. The separation is 196 MeV/c^2, sufficiently large to make the background from $B \to h^+h'^-$ negligible within the Λ_b^0 search window, as can be seen easily from Fig. 1. The background in the Λ_b^0 search window is thus predominantly combinatoric and can be estimated from the sidebands to the right and left of the search window.

The selection criteria, including the size and position of the signal region, were determined from an optimization

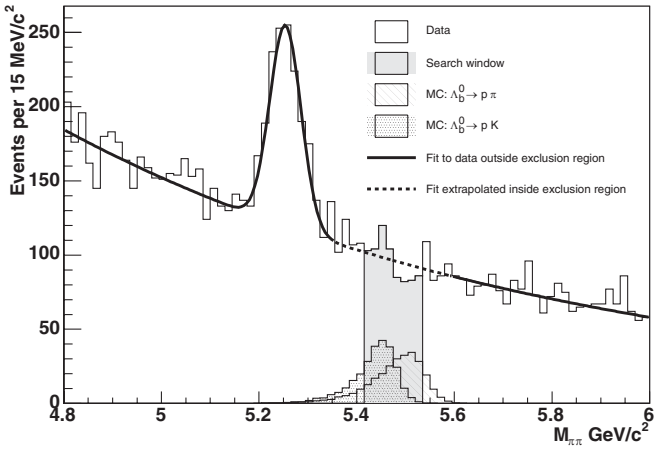

FIG. 1. Dipion invariant mass distribution of all the events including the search window. The function is the one from which we extract the number of $B \to h^+h'^-$ and background events. The dashed curve shows the fitted function in the part of the mass range that was excluded from the fit. The scales of the Monte Carlo distributions of the two signal decay modes are arbitrary. The peak in the data is given by the $B \to h^+h'^-$ events.

procedure. The sideband regions were defined to include those candidates with an invariant mass between 4.800 GeV/c^2 and 5.355 GeV/c^2 or 5.595 GeV/c^2 and 6 GeV/c^2. In the optimization procedure, we take half the candidate events in the sideband regions and maximize a figure of merit given by $S/(1.5 + \sqrt{BKG})$ [34] where S and BKG represent the number of signal and background events, respectively. The constant in the denominator is chosen to favor selections that maximize the sensitivity reach at 3σ significance. This expression reduces to the usual $S/\sqrt{BKG}$ when the background rate is large and to $S/1.5$ when the background is negligible. Hence observing that the signal is proportional to the efficiency (ϵ_Λ), in the optimization we maximize $\epsilon_\Lambda/(1.5 + \sqrt{BKG})$ where the efficiency has been evaluated using the Monte Carlo sample. We simultaneously optimize the cuts on the impact parameter of the candidate (d_Λ), its transverse decay length L_{xy}, and the minimum impact parameter of the tracks [$\min(|d_{01}|, |d_{02}|)$]. The optimal point has been found for $|d_\Lambda| < 50$ μm, $L_{xy} > 400$ μm, and $\min(|d_{01}|, |d_{02}|) > 180$ μm. The size and location of the mass search window inside the blinded region has been optimized according to the same figure of merit and spans the mass range between 5.415 GeV/c^2 and 5.535 GeV/c^2.

To estimate the expected background, we use the other half of the Λ_b^0 sideband sample and fit it to a sum of a Gaussian for the $B \to h^+h'^-$ signal and various combinations of exponential and polynomial functions for the combinatoric background. The systematic error in the yield of $B \to h^+h'^-$ and in the expected combinatoric background to the $\Lambda_b^0 \to ph^-$ signal are estimated from the spread of values obtained from different background models. Table I summarizes these as well as all other systematic uncertainties described below. As the central value we use the result obtained with the simplest model consisting of a Gaussian plus an exponential distribution. We arrive at 772 ± 31 events for the expected background in the Λ_b^0

TABLE I. List of the relative systematic error contributions to the measurement.

Affected qty.	Source	Syst. Error (%)
$B \to h^+h'^-$ yield	Bkg. shape	5.7
Bkg. estimate	Bkg. shape	3.3
$\epsilon_{\Lambda_b^0}/\epsilon_B$	$(\Lambda_b^0 \to p\pi)/(\Lambda_b^0 \to pK)$	3.5
	Window position	1.2
	Window width	9
	Lifetime	3.6
	proton's trigger efficiency	6
	$p_T(\Lambda_b^0)$	17
	Overall	21
$\mathcal{B}(B_d \to K\pi)$		5.9
f_Λ/f_d		16

search window, and 726 ± 82 events for the $B \to h^+ h'^-$ yield. Uncertainties here include both the statistical and systematic errors.

To calculate the $\mathcal{B}(\Lambda_b^0 \to ph^-)$ we need not only the event yields from the data but also the ratio of the efficiencies $\epsilon_B/\epsilon_\Lambda$ which we evaluate using Monte Carlo samples of $\Lambda_b^0 \to ph^-$ and $B_d^0 \to K\pi$. The efficiency ϵ_Λ was evaluated assuming that both $\Lambda_b^0 \to p\pi$ and $\Lambda_b^0 \to pK$ contribute with the same weight to the signal. We estimate a systematic uncertainty of 3.5%, allowing for all possible values for the ratio of branching fractions. The efficiency ratio is also sensitive to the lifetime of the b hadron, because the trigger event selection depends on the vertex displacement. In the simulation, lifetime values from PDG [28] have been used. We varied the lifetime values within the experimental uncertainty and observe a variation in the efficiency ratio of 3.6%. We quote this as a systematic error.

We assign additional systematic uncertainties due to possible discrepancies between Monte Carlo and data with regard to invariant mass scale, mass resolution, and specific ionization in the COT for different particle species. The resulting discrepancies in the mass distribution are of order a few MeV/c^2 and influence signal efficiency via the position and width of the search window. Varying position and width of the search window to reflect the measured differences of data and Monte Carlo leads to variations in signal efficiency of 1.2% and 9%, respectively.

A third source of systematic error is the variation of trigger efficiency with particle species, which arises from a different ionization energy loss in the tracking chamber. We evaluated this effect by adjusting the efficiency for pions and kaons using corrections obtained from data. As protons and kaons have similar ionization in the momentum range of interest, the efficiency for both has been corrected in the same way. After the correction, the overall variation of the relative efficiency of 6% was taken as the systematic error from this source.

The main contribution to the systematic error comes from the potential difference in p_T spectra between b mesons and Λ_b^0. As the Λ_b^0 p_T spectrum is not well measured, we use the b hadron spectrum from [20] and assume that all hadrons (mesons and baryons) have the same spectrum. We compare the efficiency for the integrated spectrum with the efficiencies for two specific p_T values. As specific p_T values we use the mean of the b meson p_T distribution, and the mean p_T of the combinatoric background events below the search window. We assign a 17% systematic error based on the spread among these three efficiency estimates.

The value of the efficiency ratio $\epsilon_B/\epsilon_\Lambda$, corrected for the trigger efficiency of different particles, is 1.77 ± 0.37, where the error includes both statistical and systematic errors. The measured value of the factor A is $(3.2 \pm 1.0) \times 10^6$, where statistical and systematic uncertainties are included, in addition to uncertainties on $\mathcal{B}(B_d^0 \to K\pi)$ and on the production fractions (f_d and f_Λ) [Eq. (2)]. The fraction of $B_d^0 \to K\pi$ [R in Eq. (2)] is calculated and the result is 0.59 ± 0.04.

The total number of events in the signal region of the mass spectrum is 767, consistent within the error with the predicted background, 772 ± 31. Because there is no excess of signal over the predicted background, we calculate upper limits on the number of signal events and the branching ratio using a Bayesian method with uniform prior distribution. This method takes into account the effect of statistical and systematic uncertainties. The resulting upper limits on the number of signal events and on $\mathcal{B}(\Lambda_b^0 \to ph^-)$ are, respectively, 75 and 2.3×10^{-5} at 90% C.L and 97 and 2.9×10^{-5} at 95% C.L. This is a significant improvement over the previously published limit of 5×10^{-5} at 90% C.L for both decay modes [17]. Substantially more statistics and improved background suppression is needed to reach the level of $1 - 2 \times 10^{-6}$ as predicted for the branching fractions in these decays in the standard model.

We thank M. Gronau, J. Rosner, I. Stewart, and Wei-Shou Hou for their comments. We thank the Fermilab staff and the technical staffs of the participating institutions for their vital contributions. This work was supported by the U.S. Department of Energy and National Science Foundation; the Italian Istituto Nazionale di Fisica Nucleare; the Ministry of Education, Culture, Sports, Science and Technology of Japan; the Natural Sciences and Engineering Research Council of Canada; the National Science Council of the Republic of China; the Swiss National Science Foundation; the A. P. Sloan Foundation; the Bundesministerium für Bildung und Forschung, Germany; the Korean Science and Engineering Foundation and the Korean Research Foundation; the Particle Physics and Astronomy Research Council and the Royal Society, United Kingdom; the Russian Foundation for Basic Research; the Comisión Interministerial de Ciencia y Tecnología, Spain; in part by the European Community's Human Potential Programme under Contract No. HPRN-CT-2002-00292; and the Academy of Finland.

[1] R. Fleischer, hep-ph/0011323.
[2] J. L. Rosner, hep-ph/0011355.
[3] M. Battle *et al.* (CLEO Collaboration), Phys. Rev. Lett. **71**, 3922 (1993).
[4] R. Godang *et al.* (CLEO Collaboration), Phys. Rev. Lett. **80**, 3456 (1998).
[5] C.-W. Chiang, M. Gronau, J. L. Rosner, and D. A. Suprun, Phys. Rev. D **70**, 034020 (2004).
[6] C. W. Bauer, I. Z. Rothstein, and I. W. Stewart, Phys. Rev. Lett. **94**, 231 802 (2005).
[7] M. Beneke, G. Buchalla, M. Neubert, and C. T. Sachrajda, Phys. Rev. Lett. **83**, 1914 (1999).
[8] I. Dunietz, Z. Phys. C **56**, 129 (1992).
[9] B. Aubert *et al.* (*BABAR* Collaboration), Phys. Rev. Lett. **93**, 131 801 (2004).
[10] Y. Chao *et al.* (Belle Collaboration), Phys. Rev. Lett. **93**, 191 802 (2004).
[11] F. Abe *et al.* (CDF Collaboration), Phys. Rev. D **55**, 1142 (1997).
[12] P. Abreu *et al.* (DELPHI Collaboration), Phys. Lett. B **374**, 351 (1996).
[13] R. Barate *et al.* (ALEPH Collaboration), Eur. Phys. J. C **2**, 197 (1998).
[14] P. Abreu *et al.* (DELPHI Collaboration), Eur. Phys. J. C **10**, 185 (1999).
[15] K. Ackerstaff *et al.* (OPAL Collaboration), Phys. Lett. B **426**, 161 (1998).
[16] R. Mohanta, A. K. Giri, and M. P. Khanna, Phys. Rev. D **63**, 074001 (2001).
[17] D. Buskulic *et al.* (ALEPH Collaboration), Phys. Lett. B **384**, 471 (1996).
[18] G. Punzi, in *Proceedings of the 32nd International Conference on High-Energy Physics (ICHEP 04)*, hep-ex/0504045.
[19] S. Klimenko, J. Konigsberg, and T. M. Liss, Fermilab Report No. FN-0741, 2003.
[20] D. Acosta *et al.* (CDF Collaboration), Phys. Rev. D **71**, 032001 (2005).
[21] A. Sill *et al.*, Nucl. Instrum. Methods Phys. Res., Sect. A **447**, 1 (2000).
[22] T. Affolder *et al.*, Nucl. Instrum. Methods Phys. Res., Sect. A **453**, 84 (2000).
[23] T. Affolder *et al.*, Nucl. Instrum. Methods Phys. Res., Sect. A **526**, 249 (2004).
[24] CDF uses a cylindrical coordinate system in which ϕ is the azimuthal angle, r is the radius from the nominal beam line and z points in the proton beam direction and is zero at the center of the detector. The transverse plane is the plane perpendicular to the z axis. The pseudorapidity η is defined as $\eta \equiv -\ln(\tan(\theta/2))$, where θ is the polar angle measured from z axis.
[25] C. S. Hill, Nucl. Instrum. Methods Phys. Res., Sect. A **530**, 1 (2004).
[26] E. J. Thomson *et al.*, IEEE Trans. Nucl. Sci. **49**, 1063 (2002).
[27] W. Ashmanskas *et al.*, Nucl. Instrum. Methods Phys. Res., Sect. A **518**, 532 (2004).
[28] S. Eidelman *et al.*, Phys. Lett. B **592** 1 (2004).
[29] S. Eidelman *et al.*, Phys. Lett. B **592**, 713 (2004).
[30] J. Abdallah *et al.* (DELPHI Collaboration), Phys. Lett. B **576**, 29 (2003).
[31] R. Barate *et al.* (ALEPH Collaboration), Eur. Phys. J. C **5**, 205 (1998).
[32] T. Affolder *et al.* (CDF Collaboration), Phys. Rev. Lett. **84**, 1663 (2000).
[33] R. Brun, R. Hagelberg, M. Hansroul, and J. C. Lasalle, CERN Reports No. CERN-DD-78-2-REV and CERN-DD-78-2.
[34] G. Punzi, *Proceedings of PhyStat2003 (SLAC, 2003)*, eConf C030908, MODT002 (2003).